ChemComm

COMMUNICATION

View Article Online
View Journal

Cite this: DOI: 10.1039/c5cc02332g

Received 19th March 2015,
Accepted 28th May 2015

DOI: 10.1039/c5cc02332g

www.rsc.org/chemcomm

Side-on cupric–superoxo triplet complexes as competent agents for H-abstraction relevant to the active site of PHM†

B. N. Sánchez-Eguía,[a] M. Flores-Alamo,[b] M. Orio[cd] and I. Castillo*[a]

Copper complexes with N_3S donors mimic the Cu_M site of copper monooxygenases and react with O_2 affording side-on cupric–superoxo complexes capable of H-abstraction from dihydroanthracene and THF. Spectroscopic and DFT data of the Cu–superoxos support a spin triplet ground state for the side-on complexes, as well as a hemilabile thioether.

Dioxygen activation by earth-abundant copper in chemical and biochemical systems is an intense area of research due to its relevance in the functionalisation of a wide range of substrates:[1] understanding the intimate details of O_2 activation at copper centres may lead to the efficient use of dioxygen in selective oxidative transformations. In copper enzymes, the readily accessible Cu^{2+}/Cu^{+} redox couple is involved in the selective oxidation of hydrocarbons,[1d] including the hydroxylation of methane.[2] Intriguingly, some of the active sites of copper monooxygenases that activate strong aliphatic C–H bonds[3] feature methionine-derived sulfur donors in addition to the ubiquitous imidazole donors from histidine residues (His_2Met). These thioether donors present in the Cu_M sites of peptidylglycine α-hydroxylating monooxygenase (PHM), dopamine β-monooxygenase (DβM), and tyramine β-monooxygenase (TβM)[4] appear to modulate the redox potential of the Cu^{2+}/Cu^{+} couple. Nonetheless, a detailed understanding of the electronic influence of thioethers to selectively hydroxylate unactivated C–H bonds remains elusive. An additional question that arises in these systems is the inertness of the thioether moiety towards oxidation during catalytic turnover conditions that could potentially result in the corresponding sulfoxide or sulfone.

The formation of a precatalytic end-on cupric superoxo complex $[Cu_M{}^{2+}–\eta^1\text{-}O_2{}^{\bullet-}]$ has been established by X-ray crystallography (Scheme 1a),[3a] although side-on η^2-O_2-bound complexes have also been evaluated as viable intermediates responsible for C–H activation (Scheme 1b).[5] Model complexes have been designed based on the His_2Met active sites of Cu–monooxygenases to gain insight into the properties of $[Cu–O_2]$ adducts, particularly cupric superoxos. Efforts have been focused on tripodal ligands with tetradentate N_3S donor sets,[6] including a recent report on a pyridine-supported, thioether-containing $[Cu^{2+}–\eta^1\text{-}O_2{}^{\bullet-}]$ complex.[6d] Benzimidazole-based N_3S–copper complexes mimic specific aspects of monooxygenase enzymes: oxygenation of $[L^1Cu]ClO_4$ resulted in electrocatalytic $O_2{}^{\bullet-}$ formation, presumably *via* a putative Cu^{2+}–superoxo.[7] This reactivity is related to the strong σ-donor properties of benzimidazoles, which place them as closer analogues of histidine than pyridine and amine derivatives, based on the pK_a and K_{ass}

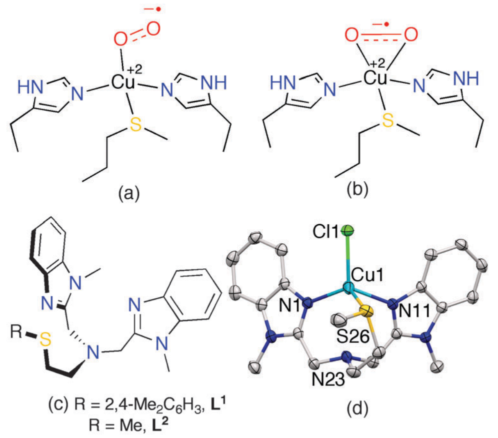

Scheme 1 (a) Precatalytic end-on Cu–superoxo $[Cu^{2+}–\eta^1\text{-}O_2{}^{\bullet-}]$ in PHM; (b) the side-on Cu–superoxo $[Cu^{2+}–\eta^2\text{-}O_2{}^{\bullet-}]$ analogue; (c) ligands employed; (d) mercury diagram of L^2CuCl at the 50% probability level; H-atoms omitted for clarity. Selected bond distances (Å): Cu1–N1 2.053(2), Cu1–N11 2.027(2), Cu1–S26 2.691(1), Cu1–Cl1 2.350(1); angles (°): N1–Cu1–N11 116.35(7), N1–Cu1–S26 123.65(5), N11–Cu1–S26 86.86(5), N1–Cu1–Cl1 112.47(5), N11–Cu1–Cl1 114.36(5), S26–Cu1–Cl1 100.29(2).

---

[a] *Instituto de Química, Universidad Nacional Autónoma de México, Circuito Exterior, CU, México DF, 04510, Mexico. E-mail: joseivan@unam.mx*

[b] *Facultad de Química, División de Estudios de Posgrado, Universidad Nacional Autónoma de México, CU, México DF, 04510, Mexico*

[c] *Laboratoire de Spectrochimie Infrarouge et Raman, Université des Sciences et Technologies de Lille, UMR CNRS 8516, 59655 Villeneuve d'Ascq Cedex, France*

[d] *Institut des Sciences Moléculaires de Marseille, Aix Marseille Université, CNRS, Centrale Marseille, ISM2 UMR 7313, 13397, Marseille, France*

† Electronic supplementary information (ESI) available: Full experimental, crystallographic, and computational details. CCDC 999325, 1036422, 1036423 and 1053447. For ESI and crystallographic data in CIF or other electronic format see DOI: 10.1039/c5cc02332g

with Cu^{2+}.[7a,8] To further establish the capability of benzimidazole-based platforms to emulate histidine donors in copper monooxygenases, we herein report a detailed study of the reactivity of O_2 with $[\mathbf{L^1}Cu]^+$ and the related $[\mathbf{L^2}Cu]^+$, featuring a methylthioether group to more closely approach the methionine donor in PHM ($\mathbf{L^1}$, $\mathbf{L^2}$: [*N*-Me-2-$CH_2(C_7H_4N_2)]_2NCH_2CH_2SR$, Scheme 1c).

Comparison of the coordination environment provided by $\mathbf{L^2}$ with the His_2Met donor set in PHM was allowed by the solid-state structure of $\mathbf{L^2}$CuCl (and its Cu^{2+} analogue, Fig. S2 in the ESI†). The complexes were obtained from the reaction of equimolar amounts of $\mathbf{L^2}$ and the appropriate copper salt. The Cu^+ centre in $\mathbf{L^2}$CuCl is in a distorted tetrahedral environment defined by benzimidazole N, thioether S, and Cl atoms, with the tertiary amine at a non-bonding distance of 2.819(2) Å (Scheme 1d). The average Cu–N bond length of 2.04 and the Cu–S distance of 2.691(1) Å are comparable to the corresponding Cu–N and Cu–S distances of 2.03 and 2.68 Å in PHM.[9] Both $\mathbf{L^1}$ and $\mathbf{L^2}$ give rise to thioether-bridged Cu^+ dimers in the solid state when non-coordinating counterions are employed ($[\mathbf{L^n}Cu]_2X_2$, $X^- = ClO_4^-$,[7a] $CF_3SO_3^-$ (OTf^-); Cu⋯Cu distances 5.407(1) and 5.055(2) Å, Fig. S3 in the ESI†).

$[\mathbf{L^n}Cu]_2OTf_2$ are nonetheless monomeric in THF solution, as corroborated by ^1H NMR spectroscopy: both complexes give rise to a single set of relatively sharp resonances for the equivalent benzimidazole groups in THF-d_8, even at −40 °C (Fig. S5, ESI†), consistent with monomeric $[\mathbf{L^n}Cu]^+$ formulations. The presence of aggregates would likely result in more than the two multiplets observed for the NCH_2CH_2S linkers between δ 3.3 and 3.5 ppm.[10d] Furthermore, DOSY NMR confirmed the monomeric nature of the complexes (Fig. S6, ESI†).

Bubbling O_2 into THF solutions of $[\mathbf{L^n}Cu]^+$ at −80 °C resulted in ESR-silent species after 15 min, with very similar optical features for both $\mathbf{L^1}$ and $\mathbf{L^2}$-complexes that are stable for at least 2 h ($\mathbf{L^1}$: λ = 336, 614 nm, $\varepsilon \sim$ 1500, 285 $M^{-1}\ cm^{-1}$; $\mathbf{L^2}$: λ = 339, 609 nm, $\varepsilon \sim$ 2300, 119 $M^{-1}\ cm^{-1}$, Fig. 1 and Fig. S12, ESI†). High energy charge transfer bands have been associated to dimeric side-on bridging peroxo complexes $[Cu^{2+}{}_2–\mu\text{-}\eta^2:\eta^2\text{-}O_2]$ with extinction coefficients >20 000 $M^{-1}\ cm^{-1}$.[11,12] Although incomplete oxygenation could account for the low apparent ε values, addition of chelating anions such as $PhCO_2^-$ or $CH_3SO_3^-$ that favour the formation of side-on peroxo dimers did not have an effect on O_2-saturated solutions of $[\mathbf{L^n}Cu]^+$ (Fig. S15 and S16, ESI†).[13,14] A better fit of the observed optical features corresponds to side-on cupric–superoxo species $[Cu^{2+}–\eta^2\text{-}O_2^{\bullet -}]$ that lack thioether bonding, similar to those reported by Tolman and coworkers (see DFT studies below).[10] Confirmation of the proposed mononuclear $[\mathbf{L^n}Cu^{2+}–\eta^2\text{-}O_2^{\bullet -}]$ formulations by resonance Raman spectroscopy was likely precluded by the photosensitivity of frozen solutions (liquid N_2, λ_{ex} 335 nm) at −125 or −80 °C in 2-MeTHF or THF, respectively. Nonetheless, the reaction of $[\mathbf{L^1}Cu]$OTf with O_2 in THF-d_8 at −80 °C was monitored by ^1H NMR spectroscopy ($[\mathbf{L^2}Cu]$OTf is considerably less soluble at this temperature). The spectrum in Fig. S12 (ESI†) reveals a single set of paramagnetically broadened signals reminiscent of the ESR-silent $[Cu(HIPT_3tren)O_2]^+$ reported by the group of Itoh,[15] and assigned as a spin triplet by Karlin, Solomon, and coworkers.[16] Signal broadening by thioether-bridged dimer formation appears to be restricted to Cu^+ complexes.[10d]

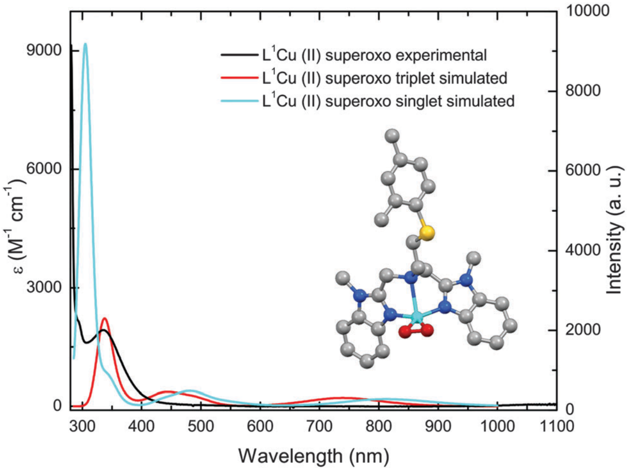

Fig. 1 Experimental UV-vis spectrum of $[\mathbf{L^1}Cu]^+$ after bubbling O_2 in THF at −80 °C (intensity in ε), and simulated spectra for triplet and singlet S-uncoordinated side-on optimised $[\mathbf{L^1}Cu\text{-}\eta^2\text{-}O_2]^+$ (intensity in a.u.). Inset: optimised structure of the triplet.

To gain insight into the bonding and electronic properties of $[\mathbf{L^n}CuO_2]^+$, DFT studies were carried out using the ORCA software package.[17] Di- and monocopper species, with and without S-bonding (N_3S *vs.* N_3 donor sets), were considered in both singlet and triplet states. Experimental data were confronted with theoretical calculations by comparing UV-vis spectra with TD-DFT results. Geometry optimisation of side-on bridging peroxos $[Cu^{2+}{}_2–\mu\text{-}\eta^2:\eta^2\text{-}O_2]$ resulted in S-uncoordinated (N_3) singlet species that gave rise to UV-vis spectra drastically different from the experimental ones (Fig. S17 and S18, ESI†), with very intense bands predicted at *ca.* 410 and 550 nm for $\mathbf{L^1}$, and 370 and 450 nm for $\mathbf{L^2}$ complexes, respectively (Fig. S19 and S20, ESI†). Optimisation of monomeric thioether-bonded complexes (N_3S) resulted in triplet end-on cupric–superoxos (Fig. S21 and S22), the singlets being higher in energy by 17 kJ mol^{-1} as expected.[16] The TD-DFT calculated data for the triplet end-on $[\mathbf{L^n}CuO_2]^+$ species differ considerably from the experimental UV-vis spectra, with absorbances at *ca.* 400 and 550 nm for $[\mathbf{L^1}CuO_2]^+$, and 475 nm for $[\mathbf{L^2}CuO_2]^+$ (Fig. S23, ESI†). Monomeric complexes with uncoordinated thioethers result in side-on structures that were analysed as singlets and triplets (Fig. 1 and Fig. S24 and S25). A better match of electronic spectra is obtained for the triplet states with respect to the experimental ones, with a strong band predicted around 340 nm, and a *d–d* band at *ca.* 740 nm (Fig. 1, red trace, and Fig. S26, ESI†); in contrast, the calculated UV-vis spectra of the singlets predict intense transitions around 300 nm (Fig. 1, blue trace). For $[\mathbf{L^1}CuO_2]^+$ an exchange coupling constant J = +250 cm^{-1} (spatial overlap S = 0.568) was obtained from BS-DFT calculations (Fig. S29, ESI†). This value shows that the two unpaired electrons of the complex are strongly ferromagnetically coupled, consistent with a triplet ground spin state that is stabilised by 6.0 kJ mol^{-1} with respect to the singlet. Similar results were obtained for $[\mathbf{L^2}CuO_2]^+$ with a calculated exchange coupling constant of +237 cm^{-1} (spatial overlap S = 0.570) consistent with a strong ferromagnetic interaction. The triplet is also the favoured ground spin state by 5.7 kJ mol^{-1} (Fig. S30 and Table S4, ESI†).

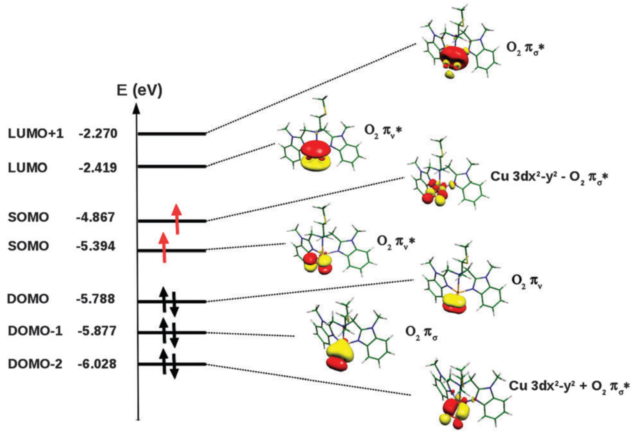

Fig. 2 Molecular orbital diagram of triplet side-on superoxo $[\mathbf{L}^2\mathrm{CuO_2}]^+$ with uncoordinated methylthioether.

For both side-on $[\mathbf{L}^n\mathrm{CuO_2}]^+$ complexes a ferromagnetic interaction is expected from an MO analysis due to the orthogonality of the two magnetic orbitals depicted in Fig. S31 and S32 (ESI†). The first one is an almost pure superoxide-centred π^*_v orbital perpendicular to the Cu–OO plane, while the second one corresponds to the antibonding interaction between the Cu $d_{x^2-y^2}$ and the π^*_σ orbitals (Fig. 2 and Fig. S33 and S34). Although side-on coordination of the superoxide anion to the Cu^{2+} centres has been associated with singlet ground states,[16] it is noteworthy in the case of $[\mathbf{L}^n\mathrm{CuO_2}]^+$ that the long, calculated Cu–O distances of 1.97 Å imply a relatively weak bond (experimental av. Cu–O distance for side-on cupric–superoxo complexes 1.84 Å).[10,18] Consequently, the bonding–antibonding interaction between the Cu $d_{x^2-y^2}$ orbitals and the superoxo π^*_σ orbitals in $[\mathbf{L}^n\mathrm{CuO_2}]^+$ is weaker than the spin-pairing energy (likely intermediate in magnitude between canonical side-on and end-on Cu–$\mathrm{O_2}$ interactions previously described),[16] resulting in a triplet ground state. The geometry around the Cu^{2+} centres is square pyramidal, with the O and N-atoms from benzimidazole donors in the basal positions (Cu–N average distance 1.96 Å), and the tertiary amine in the apical positions at a considerably longer distance (2.38 Å), defining $\mathrm{N_3}$ donor sets from $\mathbf{L}^n$ (calculated Cu···S distances 5.86 and 5.83 Å, respectively). The weak Cu–O interactions predicted for $[\mathbf{L}^n\mathrm{CuO_2}]^+$ may be ascribed to the strongly σ-donating benzimidazoles, consistent with the Natural Bond Order (NBO) analysis. The calculated Wiberg index for the Cu–N bonds is indeed larger (0.83) than that for the Cu–O bonds (0.73).[19] As a consequence, the superoxo moieties in the optimised square pyramidal triplet complexes bear a considerable amount of spin density, which may predispose them to H-abstraction.

In this context, attempts to isolate $[\mathbf{L}^n\mathrm{CuO_2}]\mathrm{OTf}$ from reactions of $[\mathbf{L}^n\mathrm{Cu}]\mathrm{OTf}$ and $\mathrm{O_2}$ in THF at −78 °C resulted in the commonly observed bridging hydroxo complexes, evidencing solvent C–H activation by the triplet side-on superoxos. Blue crystals of $[\mathbf{L}^1\mathrm{Cu}(\mu\text{-OH})]_2\mathrm{OTf}_2$ were obtained after a week, with symmetry-related Cu^{2+} centres in square pyramidal $\mathrm{N_3O_2}$ coordination environments (Cu···S distance 6.01 Å, Fig. 3). The dimers are insoluble in THF at −80 °C, with the solid-state UV-vis spectra distinct from those of $[\mathbf{L}^n\mathrm{CuO_2}]^+$, lacking the intense absorption at ∼340 nm (Fig. S42, ESI†). H-abstraction from THF by $[\mathbf{L}^2\mathrm{CuO_2}]^+$ was confirmed by UV-vis spectroscopy at −40 °C ($k = 1.78 \times 10^{-4}\ \mathrm{s^{-1}}$; $t_{1/2} = 3894$ s, Fig. S44 and S45, ESI†). The capability for C–H activation was further evaluated using 9,10-dihydroanthracene (DHA) as a H-donor. The intensity of the charge transfer band at ∼340 nm diminished over an hour with pseudo first-order behaviour upon addition of a 10-fold molar excess (3 mM solution of DHA in THF) to 0.3 mM solutions of $[\mathbf{L}^n\mathrm{CuO_2}]^+$ at −60 °C (for $\mathbf{L}^2$, $k = 0.002\ \mathrm{s^{-1}}$; $t_{1/2} = 315$ s, Fig. S45 and S46, ESI†). Dilution of the samples with 3 mL of $\mathrm{CH_2Cl_2}$, followed by quenching with 0.5 M aqueous $\mathrm{Na_2EDTA}$, evidenced the presence of anthracene and anthraquinone as oxidation products. In the case of $[\mathbf{L}^1\mathrm{CuO_2}]^+$ the products were obtained in a 1 : 1 ratio. Significantly, $[\mathbf{L}^2\mathrm{CuO_2}]^+$ is more selective for H-abstraction without further oxidation, affording the products in a 7 : 3 ratio (by GC-MS, Fig. 3 and Fig. S48 and S49, ESI†). Similar H-abstraction and further oxidation of DHA has been observed with $[\mathrm{Cu_2}^{2+}\text{–}\mu\text{-}\eta^2\text{:}\eta^2\text{-}\mathrm{O_2}]$ and $[\mathrm{Cu_2}^{3+}(\mu\text{-O})_2]$ species, albeit with longer reaction times,[11b] predominant formation of anthraquinone,[20] or the requirement for a larger excess of DHA.[21] Among cupric–superoxo complexes, singlet side-on species do not react with C–H bonds.[10,18] Triplet end-on superoxos perform H-abstraction, provided that the Cu^{2+} centres are in a tetragonal environment,[6d,22] trigonal bipyramidal (TBP) complexes being less reactive.[23] This behaviour parallels the reactivity of tetragonal cupric–hydroperoxo complexes that activate C–H bonds,[24] compared to their relatively unreactive TBP counterparts.[25] Within this context, triplet side-on complexes $[\mathbf{L}^n\mathrm{CuO_2}]^+$ fulfill the requirements for enhanced H-abstraction ability: tetragonal geometry and a triplet ground state.

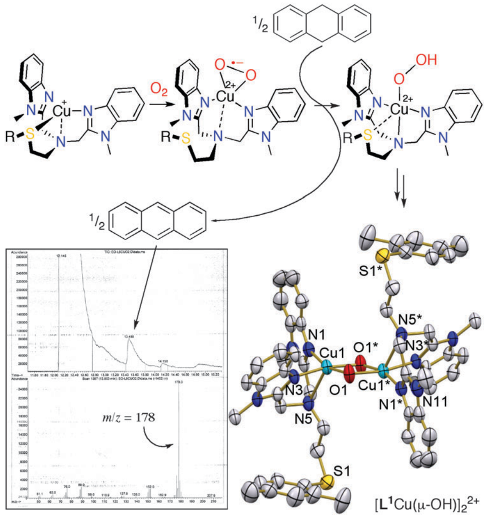

Fig. 3 Proposed reaction of $[\mathbf{L}^n\mathrm{CuO_2}]^+$ with DHA affording the final products anthracene and $[\mathbf{L}^n\mathrm{Cu}(\mu\text{-OH})]_2{}^{2+}$; Mercury diagram of $[\mathbf{L}^1\mathrm{Cu}(\mu\text{-OH})]_2{}^{2+}$ at the 50% probability level. Selected bond distances (Å): Cu1–O1 1.913(2), Cu1–O1* 1.917(3), Cu1–N1 2.006(3), Cu1–N3 1.985(2), Cu1–N5 2.460(3); angles (°): N1–Cu1–N3 96.9(1), N1–Cu1–N5 75.3(1), N3–Cu1–N5 77.0(1), N1–Cu1–O1 162.3(1), N3–Cu1–O1 93.3(1), N1–Cu1–O1* 92.3(1), N3–Cu1–O1* 168.5(1); inset: the GC-MS trace of organic products with anthracene at $m/z = 178$.

Since charge-transfer bands have been described for Cu^{2+}–hydroperoxo complexes around 360 nm,[6a,24,25a] which may form by rapid H-abstraction from solvent, we ruled out such $[\mathbf{L}^n\text{Cu–OOH}]^+$ species as the observed oxygenation products of $[\mathbf{L}^n\text{Cu}]^+$. Cu^{2+}–hydroperoxides were prepared by addition of 5–10 equiv. of 1 : 1 H_2O_2/Et_3N THF solutions to the appropriate $[\mathbf{L}^n\text{Cu}]^{2+}$ sources. In addition to being relatively stable at room temperature and ESR-active, the electronic spectra are distinct from those of $[\mathbf{L}^n\text{CuO}_2]^+$ (Fig. S35–S42, ESI†), with shoulders around 330 and 310 nm potentially due to S → Cu^{2+} charge-transfer bands of thioether-bound cupric–hydroperoxos.[6a,7] Addition of DHA to solutions of $[\mathbf{L}^n\text{Cu–OOH}]^+$ at 20–40 °C resulted in only trace amounts of oxidation products (Fig. S50 and S51, ESI†), excluding them as efficient H-abstraction agents.

In summary, benzimidazole-based N_3S ligands support side-on cupric–superoxo complexes as ground state triplets, in contrast to the prevalent view of side-on superoxos as singlets exclusively. The long Cu–O bonds opposite to the strong Cu–N σ-bonds in square pyramidal $[\mathbf{L}^n\text{Cu–}\eta^2\text{-O}_2]^+$ arise from the small overlap between the Cu $d_{x_2-y_2}$ and the O_2 π^*_σ orbitals, giving rise to the triplet ground states. Despite being strong σ-donors, benzimidazoles give rise to copper complexes that are more electrophilic than their pyridine-based analogues ($E_{1/2}$ ∼ −170 mV *vs.* Fc^+/Fc for $[\mathbf{L}^n\text{Cu}]^{+/2+}$,[7c] compared to −470 mV for pyridine-based N_3S systems).[6d] This may arise from stabilisation of Cu^+ complexes by a low-lying LUMO,[7a] setting benzimidazoles apart from related nitrogen donors, and enhancing H-abstraction. The methylthioether in $[\mathbf{L}^2\text{CuO}_2]^+$ directs H-abstraction from DHA without further oxidation, placing it as a close analogue of the Cu_M site of PHM. In this context, the thioethers are weak donors, and may even act as hemilabile ligands. Their role in triplet side-on superoxo complexes in related chemical and biochemical systems awaits further evaluation.

We thank Prof. E. I. Solomon, J. W. Ginsbach for rR; Prof. J. J. García for GC-MS; S. Hernández-Ortega for crystallography, V. Gómez-Vidales for ESR, R. Patiño for IR, M. Orta for EA, B. Quiroz, R. Gaviño for DOSY and VT-NMR, L. Ríos for ESI-MS. Funding by Conacyt (151837, 254496), PAPIIT (IN210214), IANAS.

Notes and references

1 (*a*) L. M. Mirica, X. Ottenwaelder and T. D. P. Stack, *Chem. Rev.*, 2004, **104**, 1013; (*b*) E. A. Lewis and W. B. Tolman, *Chem. Rev.*, 2004, **104**, 1047; (*c*) R. A. Himes and K. D. Karlin, *Curr. Opin. Chem. Biol.*, 2009, **13**, 119; (*d*) E. I. Solomon, D. E. Heppner, E. M. Johnston, J. W. Ginsbach, J. Cirera, M. Qayyum, M. T. Kieber-Emmons, C. H. Kjaergaard, R. G. Hadt and L. Tian, *Chem. Rev.*, 2014, **114**, 3659.

2 R. L. Lieberman and A. C. Rosenzweig, *Nature*, 2005, **434**, 177.

3 (*a*) S. T. Prigge, B. A. Eipper, R. E. Mains and L. M. Amzel, *Science*, 2004, **304**, 864; (*b*) J. P. Klinman, *J. Biol. Chem.*, 2006, **281**, 3013.

4 M. Monastirioti, C. E. Linn, Jr. and K. White, *J. Neurosci.*, 1996, **16**, 3900.

5 (*a*) P. Chen and E. I. Solomon, *J. Am. Chem. Soc.*, 2004, **126**, 4991; (*b*) P. Chen and E. I. Solomon, *Proc. Natl. Acad. Sci. U. S. A.*, 2004, **101**, 13105.

6 (*a*) M. Kodera, T. Kita, I. Miura, N. Nakayama, T. Kawata, K. Kano and S. Hirota, *J. Am. Chem. Soc.*, 2001, **123**, 7715; (*b*) L. Q. Hatcher, D.-H. Lee, M. A. Vance, A. E. Milligan, R. Sarangi, K. O. Hodgson, B. Hedman, E. I. Solomon and K. D. Karlin, *Inorg. Chem.*, 2006, **45**, 10055; (*c*) D.-H. Lee, L. Q. Hatcher, M. A. Vance, R. Sarangi, A. E. Milligan, A. A. Narducci Sarjeant, C. D. Incarvito, A. L. Rheingold, K. O. Hodgson, B. Hedman, E. I. Solomon and K. D. Karlin, *Inorg. Chem.*, 2007, **46**, 6056; (*d*) S. Kim, J. Y. Lee, R. E. Cowley, J. W. Ginsbach, M. A. Siegler, E. I. Solomon and K. D. Karlin, *J. Am. Chem. Soc.*, 2015, **137**, 2796.

7 (*a*) I. Castillo, V. M. Ugalde-Saldívar, L. A. Rodríguez Solano, B. N. Sánchez Eguía, E. Zeglio and E. Nordlander, *Dalton Trans.*, 2012, **41**, 9394; (*b*) P. R. Martínez-Alanis, B. N. Sánchez Eguía, V. M. Ugalde-Saldívar, I. Regla, P. Demare, G. Aullón and I. Castillo, *Chem. – Eur. J.*, 2013, **19**, 6067; (*c*) I. Castillo, B. N. Sánchez-Eguía, P. R. Martínez-Alanis, V. M. Ugalde-Saldívar and M. Flores-Alamo, *Polyhedron*, 2015, **85**, 824.

8 B. Ülküseven, I. Kizilcikli, A. Tavman and B. Akkurt, *Rev. Inorg. Chem.*, 2001, **21**, 369.

9 S. T. Prigge, A. S. Kolhekar, B. A. Eipper, R. E. Mains and L. M. Amzel, *Science*, 1997, **278**, 1300.

10 (*a*) D. J. E. Spencer, N. W. Aboelella, A. M. Reynolds, P. L. Holland and W. B. Tolman, *J. Am. Chem. Soc.*, 2002, **124**, 2108; (*b*) N. W. Aboelella, E. A. Lewis, A. M. Reynolds, W. W. Brennessel, C. J. Cramer and W. B. Tolman, *J. Am. Chem. Soc.*, 2002, **124**, 10660; (*c*) N. W. Aboelella, S. V. Kryatov, B. F. Gherman, W. W. Brennessel, V. G. Young, Jr., R. Sarangi, E. V. Rybak-Akimova, K. O. Hodgson, B. Hedman, E. I. Solomon, C. J. Cramer and W. B. Tolman, *J. Am. Chem. Soc.*, 2004, **126**, 16896; (*d*) N. W. Aboelella, B. F. Gherman, L. M. R. Hill, J. T. York, N. Holm, V. G. Young, Jr., C. J. Cramer and W. B. Tolman, *J. Am. Chem. Soc.*, 2006, **128**, 3445.

11 (*a*) M. J. Baldwin, D. E. Root, J. E. Pate, K. Fujisawa, N. Kitajima and E. I. Solomon, *J. Am. Chem. Soc.*, 1992, **114**, 10421; (*b*) H. V. Obias, Y. Lin, N. N. Murthy, E. Pidcock, E. I. Solomon, M. Ralle, N. J. Blackburn, Y.-M. Neuhold, A. D. Zuberbühler and K. D. Karlin, *J. Am. Chem. Soc.*, 1998, **120**, 12960; (*c*) E. Pidcock, H. V. Obias, M. Abe, H.-C. Liang, K. D. Karlin and E. I. Solomon, *J. Am. Chem. Soc.*, 1999, **121**, 1299.

12 (*a*) L. Santagostini, M. Gullotti, E. Monzani, L. Casella, R. Dillinger and F. Tuczek, *Chem. – Eur. J.*, 2000, **6**, 519; (*b*) G. Battaini, M. De Carolis, E. Monzani, F. Tuczek and L. Casella, *Chem. Commun.*, 2003, 726.

13 X. Ottenwaelder, D. J. Rudd, M. C. Corbett, K. O. Hodgson, B. Hedman and T. D. P. Stack, *J. Am. Chem. Soc.*, 2006, **128**, 9268.

14 Y. Funahashi, T. Nishikawa, Y. Wasada-Tsutsui, Y. Kajita, S. Yamaguchi, H. Arii, T. Ozawa, K. Jitsukawa, T. Tosha, S. Hirota, T. Kitagawa and H. Masuda, *J. Am. Chem. Soc.*, 2008, **130**, 16444.

15 Y. Kobayashi, K. Ohkubo, T. Nomura, M. Kubo, N. Fujieda, H. Sugimoto, S. Fukuzumi, K. Goto, T. Ogura and S. Itoh, *Eur. J. Inorg. Chem.*, 2012, 4574.

16 J. W. Ginsbach, R. L. Peterson, R. E. Cowley, K. D. Karlin and E. I. Solomon, *Inorg. Chem.*, 2013, **52**, 12872.

17 F. Neese, *Wiley Interdiscip. Rev.: Comput. Mol. Sci.*, 2012, **2**, 73.

18 (*a*) K. Fujisawa, M. Tanaka, Y. Moro-oka and N. Kitajima, *J. Am. Chem. Soc.*, 1994, **116**, 12079; (*b*) P. Chen, D. E. Root, C. Campochiaro, K. Fujisawa and E. I. Solomon, *J. Am. Chem. Soc.*, 2003, **125**, 466.

19 (*a*) A. E. Reed, L. A. Curtiss and F. Weinhold, *Chem. Rev.*, 1988, **88**, 899; (*b*) K. B. Wiberg, *Tetrahedron*, 1968, **24**, 1083.

20 D. Maiti, J. S. Woertink, A. A. Narducci Sarjeant, E. I. Solomon and K. D. Karlin, *Inorg. Chem.*, 2008, **47**, 3787.

21 C. Citek, B.-L. Lin, T. E. Phelps, E. C. Wasinger and T. D. P. Stack, *J. Am. Chem. Soc.*, 2014, **136**, 14405.

22 (*a*) A. Kunishita, M. Kubo, H. Sugimoto, T. Ogura, K. Sato, T. Takui and S. Itoh, *J. Am. Chem. Soc.*, 2009, **131**, 2788; (*b*) R. L. Peterson, R. A. Himes, H. Kotani, T. Suenobu, L. Tian, M. A. Siegler, E. I. Solomon, S. Fukuzumi and K. D. Karlin, *J. Am. Chem. Soc.*, 2011, **133**, 1702.

23 D. Maiti, D.-H. Lee, K. Gaoutchenova, C. Würtele, M. C. Holthausen, A. A. Narducci Sarjeant, J. Sundermeyer, S. Schindler and K. D. Karlin, *Angew. Chem., Int. Ed.*, 2008, **47**, 82.

24 T. Fujii, A. Naito, S. Yamaguchi, A. Wada, Y. Funahashi, K. Jitsukawa, S. Nagatomo, T. Kitagawa and H. Masuda, *Chem. Commun.*, 2003, 2700.

25 (*a*) A. Wada, M. Harata, K. Hasegawa, K. Jitsukawa, H. Masuda, M. Mukai, T. Kitagawa and H. Einaga, *Angew. Chem., Int. Ed.*, 1998, **37**, 798; (*b*) Y. J. Choi, K.-B. Cho, M. Kubo, T. Ogura, K. D. Karlin, J. Cho and W. Nam, *Dalton Trans.*, 2011, **40**, 2234.